Applied Surface Science 422 (2017) 221–227

Contents lists available at ScienceDirect

Applied Surface Science

journal homepage: www.elsevier.com/locate/apsusc

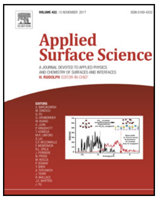

Full Length Article

CeLa enhanced corrosion resistance of Al-Cu-Mn-Mg-Fe alloy for lithium battery shell

Jiandi Du[a], Dongyan Ding[a,*], Wenlong Zhang[a], Zhou Xu[a], Yongjin Gao[b], Guozhen Chen[b], Weigao Chen[b], Xiaohua You[b], Renzong Chen[c], Yuanwei Huang[c], Jinsong Tang[c]

[a] School of Materials Science and Engineering, Shanghai Jiao Tong University, Shanghai 200240, China
[b] Huafon NLM Al Co., Ltd, Shanghai 201506, China
[c] Shanghai Huafon Materials Technology Institute, Shanghai 201203, China

ARTICLE INFO

Article history:
Received 21 March 2017
Received in revised form 27 May 2017
Accepted 2 June 2017
Available online 4 June 2017

Keywords:
Al-Cu-Mn-Mg-Fe alloy
CeLa addition
Potentiodynamic polarization
Electrochemical impedance spectroscopy

ABSTRACT

Effects of CeLa addition on the localized corrosion and electrochemical corrosion behavior of Al-Cu-Mn-Mg-Fe lithium battery shell alloy were investigated by immersion testing and electrochemical testing in 0.6 M NaCl solution at different temperatures. Experimental results indicated that CeLa addition resulted in the formation of AlCuCe/La (Al_8Cu_4Ce and Al_6Cu_6La) local cathodes and corrosion activity of the main intermetallic particles decreased in the order of Al_2CuMg, AlCuCe/La, Al_6(Mn, Fe). Corrosion potential shifted positively due to CeLa alloying. Corrosion current density of the CeLa-containing alloy was lower than that of the CeLa-free alloy at room temperature. At room temperature, there was no obvious surface passivation for both alloys. At 80 °C CeLa addition resulted in a wide passive region at the anode polarization region. Electrochemical impedance spectroscopy (EIS) analysis also indicated that corrosion resistance of the CeLa-containing alloy was much higher than that of the CeLa-free alloy.

1. Introduction

Due to excellent formability, low density and high conductivity, aluminum alloys have been extensively used as automotive radiators, heat exchangers and lithium battery shells [1–3]. With increasing application of Li-ion cell automotive industries, shell materials are required to possess preferable corrosion resistance and mechanical properties. Due to low strength, traditional 3003 alloy cannot satisfy the lightweight requirement of lithium battery shell alloy. Then, Al-Cu-Mn-Mg-Fe alloy was selected as a new kind of battery shell material, mainly due to the high specific strength [4,5] and relatively good corrosion resistance [6].

It was well known that intermetallic compounds play an important role in corrosion process for Al alloys [7]. And composition, size and number of the secondary phase particles could have a great influence on pitting corrosion [8,9]. Al_2CuMg particles could act as local anodes and may preferentially release Al and Mg according to a dealloying process in NaCl solution [10]. Then the particles would become more cathodic as a mass of Cu were remained. Leard et al. found that these intermetallic particles decreased in activity in the order of Al_2CuMg, Al_7Cu_2Fe and $Al_{20}Cu_2Mn_3$ [11]. Boag et al. found that the S-phase was attacked firstly, and then AlCuFeMn particles such as Al_7Cu_2Fe and Al_6(Cu, Mn, Fe) were attacked [12].

Corrosion resistance of aluminum alloy can be improved through rare earth Sc [13], Ce [6] and Sm [14] addition, cerium-based [15] or lanthanum-based conversion [16]. Shi et al. reported influences of Sc and Zr additions on the corrosion behavior of Al-Zn-Mg-Cu alloy. They found that addition of Sc and Zr could improve corrosion resistance by inhibiting recrystallization [13]. Zhang et al. found that Ce addition could improve corrosion resistance of Al-Cu-Mn-Mg-Fe alloy because it could suppress the formation of Al_2Cu particles [6]. We investigated the influence of CeLa addition on the microstructures and mechanical properties of Al-Cu-Mn-Mg-Fe alloy and found that the mechanical properties was greatly improved if proper amount of CeLa was added to the alloy [17].

The pitting behavior of those intermetallic phases in Al-Cu-Mn alloy has been reported in many literatures. However, effect of CeLa addition on pitting behavior and general corrosion (potentiodynamic polarization, EIS and mass loss) of Al-Cu-Mn-Mg-Fe alloy was rarely reported. In this work, pitting corrosion through immersion testing and electrochemical corrosion of CeLa-containing alloy were investigated to evaluate the effect of CeLa addition on corrosion behavior of the alloy. Since the temperature of lithium battery shell may increase during charging or discharging process, potentiodynamic polarization was also carried out at 50 °C and 80 °C.

---

* Corresponding author.
E-mail address: dyding@sjtu.edu.cn (D. Ding).

http://dx.doi.org/10.1016/j.apsusc.2017.06.013
0169-4332/

Table 1
Chemical compositions of the experimental alloys (wt.%).

Alloy	Cu	Mn	Mg	Fe	Ce	La	Al
Al-Cu-Mn-Mg-Fe	1.48	1.33	0.74	0.53	0	0	Bal.
Al-Cu-Mn-Mg-Fe-0.25 CeLa	1.49	1.35	0.75	0.54	0.14	0.13	Bal.

2. Experimental

2.1. Materials preparation

The prepared ingots were successively heated to 590 °C at a heating rate of 15 °C/min, and held in the isothermal condition for 8 h, followed by cooled until to room temperature (25 °C). The homogenized ingots with a thickness of 40 mm were preheated at 500 °C and then hot rolled to 3 mm-thick plates. The prepared hot rolled plates were stress-relief annealing at 300 °C for 2 h, and cold rolled to 0.45 mm sheets. The sheets were finally annealed at 150 °C for 24 h. The low temperature annealing can improve the ductility and formability, which is helpful for subsequent processing [18]. Chemical composition of the experimental alloys was analyzed by inductively coupled plasma-optical emission spectroscopy (ICP-OES) and corresponding results were listed in Table 1.

2.2. Microstructural characterization

The microstructures of the alloys were investigated by a field-emission scanning electron microscope (SEM, JSM-7600F, JEOL) with a resolution of 1.0 nm (15 KV) and a field-emission transmission electron microscope (TEM, JEM-2100F, JEOL) with a point resolution of 0.19 nm. SEM investigations were performed at the accelerating voltage of 15 kV and probe current of 2×10^{-10} A with a working distance of about 8 mm (scanning mode of backscattered electron mode). Energy dispersive spectroscope (EDS) was used to identify the compositions of different intermetallic compounds at the accelerating voltage of 20 kV with a working distance of 15 mm. TEM samples were electro-polished in 4% $HClO_4$ and ethanol solutions at −30 °C, followed by an ion beam thinning. TEM observations were performed at the accelerating voltage of 200 kV and emission current of around 195 μA.

2.3. Immersion corrosion and mass loss testing

Immersion corrosion experiment was conducted following Chinese National Standards (JB/T 7901-1999). Polished specimens with a size of 10 mm × 10 mm were immersed in 0.6 M NaCl solution at room temperature in free air for different time varying from 2.5 min to 144 h. Corrosion surfaces of the specimens were investigated with SEM attached with EDS to determine distribution of alloying elements.

Polished specimens with a size of 20 mm × 20 mm were rinsed successively by acetone, ethanol and distilled water, and finally dried in air. The specimens were immersed in 0.6 M NaCl solution at room temperature for different time (1, 4, 6, 10, 20 and 30 days). Corrosion products were removed by chemical cleaning with 15% HNO_3 [19]. The mass of the specimens before and after immersion was measured by using an analytical balance (FA124) with a precision of 0.1 mg. Each mass loss measurement was repeated for three times.

2.4. Electrochemical measurements

Electrochemical measurements were performed on a CHI 660E electrochemical system by using a three electrode cell. The working electrode, reference electrode and counter electrode were specimen, Ag/AgCl (0.1 M KCl) and a Pt wire, respectively. The work electrode was in size of 10 mm × 10 mm. All of the electrochemical tests were conducted with 0.6 M NaCl solution in free air. Specimens for potentiodynamic polarization testing were conducted at a scanning rate of 1 mV/s, ranging from −1 V to 0 V. The testing temperature was room temperature (25 °C), 50 °C and 80 °C, respectively. The electrode potentials were converted to standard hydrogen electrode (SHE) according to the following equation [20].

$$E_{SHE} = E_{obs} + 0.2866 - 0.001(T\text{-}T_0) + 1.745 \times 10^{-7} (T\text{-}T_0)^2 - 3.03 \times 10^{-9}(T\text{-}T_0)^3 \quad (1)$$

where E_{SHE} represents the electrode potential vs. SHE. E_{obs} represents the measured electrode potential. T represents the experimental temperature and T_0 represents the room temperature (25 °C).

Using the same device for the potentiodynamic polarization testing, EIS testing were conducted at open circuit potential (E_{corr}) with a frequency ranging from 100 KHz to 10 mHz, using a perturbation voltage of 5 mV. The testing temperature was 25 °C. Zsimpwin software was used for fitting of the impedance spectra. Every potentiodynamic polarization and EIS measurements was repeated at least three times to obtain a stable testing value.

3. Results and discussion

3.1. Microstructural characterization

Fig. 1 shows backscattered electron images of the alloys with and without CeLa addition. A large many of grey phases (particles A) with irregular shape could be found in the two alloys and some white phases (particles B) appeared in the CeLa-containing alloy. The grey phases were confirmed as Al_6(Mn, Fe) and the white phases were AlCuCe/La (Al_8Cu_4Ce and Al_6Cu_6La), according to our previous work [17]. The Al_6(Mn, Fe) could be refined when CeLa was added to the Al-Cu-Mn-Mg-Fe alloy, which helped to enhance mechanical properties of the alloy [17] and may also affect the corrosion properties of the relevant alloys.

Fig. 2 shows TEM images of the alloys with and without CeLa addition. The plate-like particles were Al_2CuMg (S) phase and the rod-like particles were $Al_{20}Cu_2Mn_3$ (T) phase [17,21]. Statistical analysis and Rietveld refinement indicated that the volume fraction of T phase increased and S phase decreased as CeLa was added to the Al-Cu-Mn-Mg-Fe alloy [17]. As the S phase and T phase have different corrosion properties [22,23], the difference in volume fraction of the two phases should have a strong influence on the electrochemical corrosion property of the above alloys.

3.2. Immersion corrosion and mass loss analysis

Fig. 3 shows backscattered electron images of CeLa-containing alloy after immersion in 0.6 M NaCl solution for 2.5, 10, 30 min and 6 h. It could be found that extensive tiny second phase particles were corroded after 2.5 min immersion. These particles appeared as round shape in the size of about hundreds of nanometers. According to the intermetallic particles analysis in Fig. 2, these particles should be S-phase (Al_2CuMg). Peripheral particles along the phase/matrix border were firstly eroded. The particles were gradually eroded from periphery to inside, with the extension of immersion time. A lot of corrosion pits appeared on the surface as the S-phase particles were dealloying when the immersion time was up to 10 min, and there was no obvious evidence that other second phase particles were attacked. The above results indicated that S-phase particles firstly begun the process of dealloying. The reason was